# Nodal-Antinodal Dichotomy and the Two Gaps of a Superconducting Doped Mott Insulator

M. Civelli,[1] M. Capone,[2] A. Georges,[3] K. Haule,[4] O. Parcollet,[5] T. D. Stanescu,[6] and G. Kotliar[4]

[1]*Theory Group, Institut Laue Langevin, Grenoble, France*
[2]*SMC, CNR-INFM, and Physics Department, University of Rome "La Sapienza," Piazzale Aldo Moro 5, I-00185, Rome, Italy*
*and ISC-CNR, Via dei Taurini 19, I-00185, Rome, Italy*
[3]*Centre de Physique Théorique, CNRS, Ecole Polytechnique, 91128 Palaiseau Cedex, France*
[4]*Physics Department and Center for Materials Theory, Rutgers University, Piscataway, New Jersey 08854-8019, USA*
[5]*Service de Physique Théorique, CEA/DSM/SPhT-CNRS/SPM/URA 2306 CEA-Saclay, F-91191 Gif-sur-Yvette, France*
[6]*Condensed Matter Theory Center, Department of Physics, University of Maryland, College Park, Maryland 20742-4111, USA*

We study the superconducting state of the hole-doped two-dimensional Hubbard model using cellular dynamical mean-field theory, with the Lanczos method as impurity solver. In the underdoped regime, we find a natural decomposition of the one-particle (photoemission) energy gap into two components. The gap in the nodal regions, stemming from the anomalous self-energy, decreases with decreasing doping. The antinodal gap has an additional contribution from the normal component of the self-energy, inherited from the normal-state pseudogap, and it increases as the Mott insulating phase is approached.

Superconductivity in strongly correlated materials such as the high-$T_c$ cuprates has been the subject of intensive research for more than 20 years (for a review, see, e.g., [1]). From the theoretical side, low-energy descriptions in terms of quasiparticles interacting with bosonic modes have been widely studied starting from the weak correlation limit. A different approach views the essence of the high-$T_c$ phenomenon as deriving from doping with holes a Mott insulator [2]. The strong correlation viewpoint has not been yet developed into a fully quantitative theory and whether the weak- and strong-coupling pictures are qualitatively or only quantitatively different is an important open issue.

The development of dynamical mean-field theory (DMFT) and its cluster extensions [3] provides a new path to investigate strongly correlated systems. These methods construct a mean-field theory for Hubbard-like models using a cluster of sites embedded in a self-consistent bath. Extensive investigations have been carried out for intermediate interaction strength using the dynamical cluster approximation on large clusters [4]. The strong-coupling limit is more difficult, as only small clusters can be employed. Many groups, however, have identified interesting phenomena, such as the competition between superconductivity and antiferromagnetism [5], the presence of a pseudogap (PG) [6], the formation of Fermi arcs [7–10], and the existence of an avoided critical point [11]. In this work we use cellular DMFT (CDMFT) to explore the energy gap in the one-particle spectra of the superconducting state when correlations are strong. The goal is to identify qualitative aspects of the approach to the Mott transition in the light of recent experimental studies on superconducting underdoped cuprates [12–16], which report the presence of two distinct energy scales.

We consider the two-dimensional Hubbard model:

$$\mathcal{H} = -\sum_{i,j,\sigma} t_{ij} c_{i,\sigma}^\dagger c_{j,\sigma} + U \sum_i n_{i\uparrow} n_{i\downarrow} \qquad (1)$$

$c_{i,\sigma}$ destroys a $\sigma$-spin electron on site $i$, $n_{i\sigma} = c_{i\sigma}^\dagger c_{i\sigma}$ is the number operator, and $t_{ii} \equiv \mu$ is the chemical potential. Only next-neighbor $t$ and nearest-next-neighbor $t' = -0.3t$ hoppings are considered. The on-site repulsion is set $U = 12t$. We implement CDMFT on a $2 \times 2$ plaquette. Though this is the minimal configuration allowing to study a $d$-wave superconducting state, it already presents a rich physics and we think that its deep understanding is an essential step to be accomplished before challenging bigger clusters (hardly accessible by the computational methods presently available). $\mathcal{H}$ is mapped onto a $2 \times 2$ cluster Anderson impurity model which is solved using the Lanczos method [17]. The CDMFT self-consistency condition [18] is then enforced via the Dyson relations $\hat{\Sigma}(i\omega_n) = \hat{\mathcal{G}}^{-1}(i\omega_n) - \hat{G}^{-1}[\hat{\Sigma}](i\omega_n)$, which determines the cluster self-energy $\hat{\Sigma}$. The hat denotes $8 \times 8$ matrices with cluster-site indices containing both normal and anomalous components (Nambu notation). $\hat{\mathcal{G}}$ is the "Weiss field" describing the bath, $\hat{G}[\hat{\Sigma}]$ is the one-particle cluster Green's function [18], and $\omega_n = (2n + 1)\pi/\beta$ the Matsubara frequencies, with $\beta t = 300$. The bath is described by 8 energy levels determined through a fit on the Matsubara axis ($0 < \omega_n < 2U$), which weights more the low frequencies [8].

Our main result is the presence of two energy scales on the underdoped side of the phase diagram. We first show that this can be established directly from an analysis of quantities inside the $2 \times 2$ cluster, which are the output of the CDMFT procedure. In the left panel of Fig. 1 we
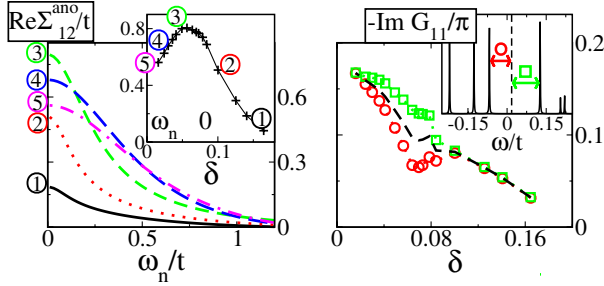
FIG. 1 (color online).   Left: $\mathrm{Re}\Sigma_{12}^{\mathrm{ano}}$ vs $\omega_n$. In the inset, the $\omega_n \to 0$ value as a function of doping $\delta$. Right: The distance from the Fermi level ($\omega = 0$) of the left (circle) and right (square) edge-peaks in the local DOS $-\frac{1}{\pi}\mathrm{Im}G_{11}$ (see inset) are displayed as a function of $\delta$. The dashed line is the average of the left and right values. In the inset $G_{11}$ is shown for $\delta = 0.06$ using a broadening $\eta \sim 7 \times 10^{-3}t$ to display poles.

display the real part of the anomalous cluster self-energy $\Sigma^{\mathrm{ano}}$ on the Matsubara axis. Only the nearest-neighbor component $\mathrm{Re}\Sigma_{12}^{\mathrm{ano}}(i\omega)$ is appreciably nonzero. The main observation is that at low energy $\Sigma_{12}^{\mathrm{ano}}(0)$ presents a non-monotonic behavior with doping $\delta$, as emphasized in the inset. A first characteristic energy scale, measuring the superconducting contribution to the one-particle energy gap, can be defined as $Z_{\mathrm{nod}}\Sigma_{12}^{\mathrm{ano}}(0)$, where $Z_{\mathrm{nod}}$ is the quasiparticle spectral weight at the nodal $k$ points, where quasiparticles are well defined. As shown below, and as physically expected, $Z_{\mathrm{nod}}$ decreases as the doping is reduced towards the Mott insulator. Hence, $Z_{\mathrm{nod}}\Sigma_{12}^{\mathrm{ano}}(0)$ decreases too due to the behavior of both $Z_{\mathrm{nod}}$ and $\Sigma_{12}^{\mathrm{ano}}(0)$. We stress the sharp contrast of this result with resonating valence bond mean-field (RVBMF) theories [19], where $Z_{\mathrm{nod}}\Sigma_{12}^{\mathrm{ano}}(0)$ corresponds to the spinon pairing amplitude which is largest close to half-filling. In the right panel of Fig. 1 we show that there is actually another energy scale, which increases when the doping level is reduced. This is revealed by looking at the local density of state (DOS) $-\frac{1}{\pi}\mathrm{Im}G_{11}$ in $\hat{G}[\hat{\Sigma}]$. In the Lanczos CDMFT the spectral function on the real axis is obtained as a discrete set of poles (shown in the inset), which are displayed by adding a small imaginary broadening $i\eta$. We extract relevant energy scales by measuring the distance from the Fermi level of the gap edge peaks. While for $\delta > 0.08$ the spectrum is symmetric, an asymmetry appears for $\delta < 0.08$. The total energy gap (dashed line in Fig. 1) grows with decreasing doping $\delta$, as in RVBMF theories.

In order to make contact with experimental observables it is useful to obtain momentum-resolved quantities from the local cluster quantities. For this we need a periodization procedure restoring the translational invariance of the lattice. Several schemes have been proposed [3]. Building on previous normal-state studies [7,9] we use a mixed scheme which is able to reconstruct the local cluster Green's function (upon integrating over $k$ the lattice Green's function) in the nodal and antinodal points better than uniform periodization schemes. Our method is based on the idea

that, when the self-energies are regular, the most suitable choice is to periodize the cluster self-energy via the formula

$$\Sigma_\sigma(k, \omega) = \frac{1}{N_c}\sum_{\mu\nu}e^{-ik\mu}\Sigma_{\mu\nu,\sigma}(\omega)e^{ik\nu} \qquad (2)$$

($\mu$, $\nu$ label cluster sites). The anomalous self-energy $\Sigma^{\mathrm{ano}}$ and the normal self-energy $\Sigma^{\mathrm{nor}}$ *in the nodal regions*, where we expect to find quasiparticles, are well behaved quantities, therefore we extract them through formula (2). In particular, the anomalous self-energy acquires a standard $d_{x^2-y^2}$-wave form: $\Sigma^{\mathrm{ano}}(k, \omega) = \Sigma_{12}^{\mathrm{ano}}(\omega)(\cos k_x - \cos k_y)$. On the other hand, when the self-energies develop singularities, the cluster self-energy is not a good quantity to be periodized. In Ref. [9], it has been shown that this takes place in the normal self-energy $\Sigma^{\mathrm{nor}}$ *in the antinodal regions*, when the system approaches the Mott insulator. In this case, a more suitable quantity to be periodized is the irreducible two-point cluster cumulant $\mathcal{M}_\sigma^{\mathrm{nor}}(\omega) = [(\omega + \mu)\hat{1} - \hat{\Sigma}_\sigma^{\mathrm{nor}}]^{-1}$, which is a more local and regular quantity. In the antinodal region, therefore, we can apply formula (2) to $\mathcal{M}^{\mathrm{nor}}$, to obtain $\mathcal{M}^{\mathrm{nor}}(k, \omega)$ and finally extract the normal lattice self-energy $\Sigma^{\mathrm{nor}}(k, \omega) = \omega + \mu - 1/\mathcal{M}^{\mathrm{nor}}(k, \omega)$. The $k$-dependent Green's function can be written as a matrix in Nambu's space.

$$\hat{G}_{k\sigma}^{-1}(\omega) = \begin{pmatrix} \omega - t_k - \Sigma_\sigma^{\mathrm{nor}}(k, \omega) & -\Sigma^{\mathrm{ano}}(k, \omega) \\ -\Sigma^{\mathrm{ano}}(k, \omega) & \omega + t_k + \Sigma_\sigma^{\mathrm{nor}}(k, -\omega)^* \end{pmatrix}.$$
$$(3)$$

The imaginary part of the diagonal entry yields the spectral function $A(k, \omega)$ measured in photoemission.

In order to compare our results with experiments, it is useful to disentangle the normal and superconducting contributions to the spectral gap. To this end, we first set $\Sigma^{\mathrm{ano}} = 0$ in Eq. (3). The results are shown in Fig. 2. The $k$ points along the nodal and antinodal directions are chosen as those where the highest peak is observed in $A(k, \omega)$, as done, e.g., in Ref. [13]. Their actual values are shown in the inset of panel C of Fig. 2. Near the nodal point (panel A) a quasiparticle peak is well defined at the Fermi level ($\omega = 0$) and decreases by decreasing doping. In the antinodal region (panel B), a quasiparticle peak is also found at the Fermi level for $\delta > 0.08$. For $\delta < 0.08$, however, the spectral weight shifts to negative energies signaling the opening of a PG, whose size increases as $\delta \to 0$. The behavior of the PG in the superconducting solution smoothly connects to the PG previously found in the normal-state CDMFT study [9]. The approach to the Mott transition is characterized by a strong reduction in the area of the nodal spectral peak $Z_{\mathrm{nod}}$, which is plotted in panel C (green circles). We also plot the area of the anti-nodal peak $Z_{\mathrm{anod}}$, which shows a constant value upon the opening of the PG ($\delta > 0.08$). In panel D, we restore $\Sigma^{\mathrm{ano}}$, and examine the actual superconducting solution. The superconducting gap opens in the antinodal region (the
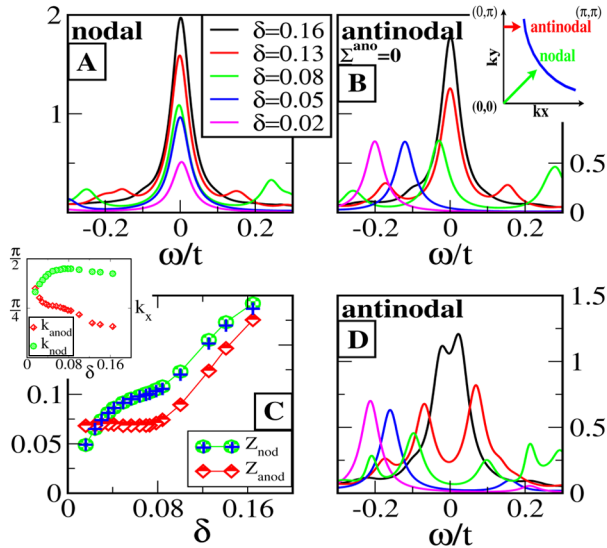
FIG. 2 (color online). Spectral function $A(k, \omega)$ for different $\delta$. Broadening $\eta = 0.03t$. Panel A: nodal-quasiparticle peak; panel B, normal component [set $\Sigma^{\text{ano}} = 0$ in Eq. (3)] of the antinodal quasiparticle peaks; panel C, nodal and antinodal quasiparticle weights. The inset shows the $k$ positions of the nodal and antinodal points; panel D, spectra at the antinodes.



FIG. 3 (color online). Left: $v_{\text{nod}}$ and $v_\Delta$ as a function of doping $\delta$ ($a_o$ is the lattice spacing). Right: low-frequency coefficients of local DOS $\gamma$ and of the Raman $B_{2g}$ and superfluid density response $\alpha$, renormalized by the value at $\delta = 0.16$.

nodal region is practically unaffected). For $\delta > 0.08$ the spectra are almost symmetric around the Fermi level, as in a standard BCS $d$-wave superconductor. In contrast, close to the Mott transition the PG, which originates from the normal component, is superimposed to the superconducting gap, resulting in asymmetric spectra. This reveals the origin of the left-right asymmetry in the cluster DOS discussed in Fig. 1.

In the nodal region the quasiparticle peaks are well defined at all dopings and we can expand the self-energies at low frequencies. The quasiparticle residue $[1 - \partial_\omega \text{Re}\Sigma_k(\omega)]^{-1}|_{\omega=0}$ (blue crosses in panel C of Fig. 2) numerically coincides with the area of the quasiparticle peak $Z_{\text{nod}}$. From Eq. (3), we get $A(k, \omega) \simeq Z_{\text{nod}}\delta(\omega - \sqrt{v_{\text{nod}}^2 k_\perp^2 + v_\Delta^2 k_\parallel^2})$, where $v_{\text{nod}} = Z_{\text{nod}}|\nabla_k[t_k - \Sigma^{\text{nor}}(k, 0)]|$ and $v_\Delta = \sqrt{2}Z_{nod}\Sigma_{12}^{\text{ano}}(0)|\sin k_{\text{nod}}|$ are the normal and anomalous velocities, respectively, perpendicular and parallel to the Fermi surface. $v_\Delta$ physically expresses the superconducting energy-scale discussed in the left panel of Fig. 1. We display them as a function of doping $\delta$ on the left side of Fig. 3. $v_{\text{nod}}$ does not show a special trend for $\delta \to 0$ and it stays finite, consistently with experiments [20]. The anomalous velocity, $v_\Delta \ll v_{\text{nod}}$ presents a dome-like shape. This behavior (confirmed by continuous time quantum Monte Carlo (CTQMC) calculations [21]) is in agreement with recent experiments on underdoped cuprates showing that, contrary to the antinodal gap, the nodal gap decreases by reducing doping [12–14].

The low-energy behavior of several physical observables in the superconducting state is controlled by nodal-quasiparticle properties and hence can be related to $v_{\text{nod}}$,
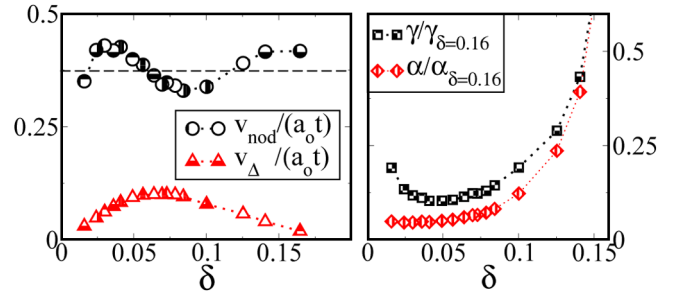
$v_\Delta$ and $Z_{\text{nod}}$. Two specific ratios are particularly significant, namely: $\gamma = Z_{\text{nod}}/(v_{\text{nod}}v_\Delta)$ and $\alpha = Z_{\text{nod}}^2/(v_{\text{nod}}v_\Delta)$. The first one is associated with the low-energy behavior of the local DOS measured in tunneling experiments: $N(\omega) = \sum_k A(k, \omega) \sim \gamma\omega$ (for $\omega \to 0$). Neglecting vertex corrections [12], the second one determines the low-energy $B_{2g}$ Raman response function $\chi''(\omega) \propto \alpha\omega$ and the low-temperature ($T \to 0$) behavior of the penetration depth (superfluid density) $\rho_s(T) - \rho_s(0) \propto \alpha T$. We display $\alpha$ and $\gamma$ in the right panel of Fig. 3 as a function of $\delta$. $\alpha$ is monotonically decreasing (see also CTQMC results [21]) and, on the underdoped side $\delta < 0.08$, it saturates to a constant value, in agreement with Raman spectroscopy [12] and penetration depth measurements [22]. Also $\gamma$ neatly decreases in going from the overdoped to the underdoped side, but it presents a weak upturn for low doping. The low-frequency linear behavior of $N(\omega)$ is well established in scanning tunneling experiments on the cuprates [23]. However, it is not currently possible to determine the absolute values of the tunneling slope $\alpha$ from experiments, hence the behavior we find is a theoretical prediction.

We finally turn to the one-electron spectra in the antinodal region, shown in Fig. 4, physically interpreting the cluster energy scales observed in Fig. 1. We evaluate the antinodal gap in the superconducting state $\Delta_{\text{tot}}$ by measuring the distance from the Fermi level ($\omega = 0$) at which spectral peaks are located (panel D of Fig. 2). $\Delta_{\text{tot}}$ monotonically increases by reducing doping, as observed in experiments. The data of panel B in Fig. 2, where $\Sigma^{\text{ano}} = 0$, allow us to extract the normal contribution $\Delta_{\text{nor}}$. We notice that the peaks found there at negative frequency $\omega_{\text{pg}}$ do not represent Landau quasiparticles in a strict sense, but we can estimate the PG as $|\omega_{\text{pg}}|$. We also display the anomalous contribution to the antinodal gap $\Delta_{\text{sc}} = \sqrt{\Delta_{\text{tot}}^2 - \Delta_{\text{nor}}^2}$, and find that, within numerical precision, $\Delta_{\text{sc}} \simeq Z_{\text{anod}}|\Sigma^{\text{ano}}(k_{\text{anod}}, \omega_{\text{pg}})|$. The appearance of $\Delta_{\text{nor}}$ signs a downturn in $\Delta_{\text{sc}}$. We interpret $\Delta_{\text{tot}}$ as the monotonically increasing antinodal gap observed in cuprate superconductors, while the superconducting gap $\Delta_{\text{sc}}$, detectable as the nodal-slope $v_\Delta$ (Fig. 3), is decreasing in approaching the Mott transition.
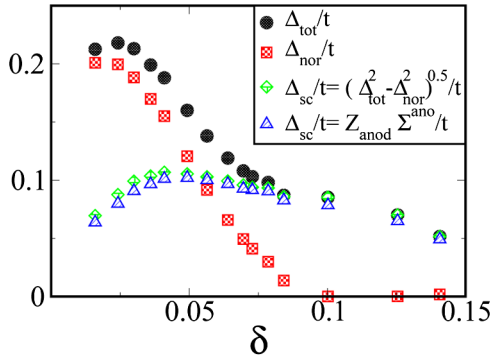
FIG. 4 (color online). Antinodal energy gap $\Delta_{tot}$ (circles), obtained from the spectra of panel D in Fig. 2, as a function of doping $\delta$, and decomposed in a normal contribution $\Delta_{nor}$ (squares), obtained from panel B in Fig. 2, and in a superconducting contribution $\Delta_{sc}$ (diamonds).

The concept of two energy gaps with distinct doping dependence in the cuprates has recently been brought into focus from an analysis of Raman spectroscopy [12], and photoemission experiments [13,14], which have revived experimental and theoretical debate [16]. Our theoretical dynamical mean-field study of superconductivity near the Mott transition establishes the remarkable coexistence of a superconducting gap, stemming from the anomalous self-energy, with a PG stemming from the normal self-energy. This is reminiscent of slave-boson RVBMF of the $t$-$J$ model [19,24], which uses order parameters defined on a link and includes the possibility of pairing in *both* the particle-particle and the particle-hole channels. Compared to the self-energy of the RVBMF, the CDMFT lattice self-energy has considerably stronger variations on the Fermi surface [9] and additional frequency dependence, which makes the electron states near the antinodes very incoherent even in the superconducting state. Furthermore, in the RVBMF theory the anomalous self-energy monotonically increases by decreasing doping, in contrast to our CDMFT results which reveal a second energy scale associated with superconductivity, distinct from the PG, which decreases with decreasing doping. Whether this feature survives in larger clusters, representing a property of the real ground-state, or it requires some further ingredient to be stabilized against competing instabilities (above all antiferromagnetism at low doping [5]) remains an important open question addressed to future developments. We think, however, that the assumption of a $d$-wave superconducting ground state is a reasonable starting point, and the importance of our $2 \times 2$ plaquette CDMFT result stands in the natural explanation it provides of the properties of underdoped cuprates.

[1] K. H. Bennemann and J. B. Ketterson, *Physics of Superconductors II* (Springer-Verlag, Berlin, 2004).
[2] P. W. Anderson, Science **235**, 1196 (1987).
[3] For reviews, see A. Georges *et al.*, Rev. Mod. Phys. **68**, 13 (1996); A.-M. S. Tremblay *et al.*, Low Temp. Phys. **32**, 424 (2006); Th. Maier *et al.*, Rev. Mod. Phys. **77**, 1027 (2005); G. Kotliar *et al.*, Rev. Mod. Phys. **78**, 865 (2006).
[4] T. A. Maier *et al.*, Phys. Rev. Lett. **95**, 237001 (2005); T. A. Maier, M. Jarrell, and D. J. Scalapino, Phys. Rev. B **75**, 134519 (2007).
[5] For discussions with different cluster methods: A. I. Lichtenstein and M. I. Katsnelson, Phys. Rev. B **62**, R9283 (2000); M. Capone and G. Kotliar, Phys. Rev. B **74**, 054513 (2006); B. Kyung and A.-M. S. Tremblay, Phys. Rev. Lett. **97**, 046402 (2006); David Sénéchal *et al.*, Phys. Rev. Lett. **94**, 156404 (2005); M. Aichhorn *et al.*, Phys. Rev. B **74**, 024508 (2006).
[6] M. Jarrell *et al.*, Europhys. Lett. **56**, 563 (2001); T. D. Stanescu and P. Phillips, Phys. Rev. Lett. **91**, 049901(E) (2003); B. Kyung *et al.*, Phys. Rev. B **73**, 165114 (2006).
[7] O. Parcollet, G. Biroli, and G. Kotliar, Phys. Rev. Lett. **92**, 226402 (2004).
[8] M. Civelli *et al.*, Phys. Rev. Lett. **95**, 106402 (2005).
[9] T. D. Stanescu and G. Kotliar, Phys. Rev. B **74**, 125110 (2006); T. D. Stanescu *et al.*, Ann. Phys. (N.Y.) **321**, 1682 (2006).
[10] C. Berthod *et al.*, Phys. Rev. Lett. **97**, 136401 (2006).
[11] K. Haule and G. Kotliar, Phys. Rev. B **76**, 092503 (2007).
[12] M. Le Tacon *et al.*, Nature Phys. **2**, 537 (2006).
[13] K. Tanaka *et al.*, Science **314**, 1910 (2006).
[14] T. Kondo *et al.*, Phys. Rev. Lett. **98**, 267004 (2007).
[15] K. K. Gomes *et al.*, Nature (London) **447**, 569 (2007).
[16] For earlier discussions of related ideas, see G. Deutscher, Nature (London) **397**, 410 (1999); B. Kyung and A.-M. S. Tremblay, arXiv:cond-mat/0204500; for more recent discussions, see K. Y. Yang, T. M. Rice, and F. C. Zhang, Phys. Rev. B **73**, 174501 (2006); A. J. Millis, Science **314**, 1888 (2006); A. Cho, Science **314**, 1072 (2006); S. Huefner *et al.*, arXiv:0706.4282; B. Valenzuela and E. Bascones, Phys. Rev. Lett. **98**, 227002 (2007); M. Aichhorn *et al.*, Phys. Rev. Lett. **99**, 257002 (2007).
[17] M. Caffarel and W. Krauth, Phys. Rev. Lett. **72**, 1545 (1994).
[18] S. S. Kancharla *et al.*, arXiv:cond-mat/0508205.
[19] See, e.g., P. A. Lee *et al.*, Rev. Mod. Phys. **78**, 17 (2006).
[20] X. J. Zhou *et al.*, Nature (London) **423**, 398 (2003).
[21] K. Haule and G. Kotliar, Phys. Rev. B **76**, 104509 (2007).
[22] D. A. Bonn *et al.*, Czech. J. Phys. **46**, 3195 (1996); C. Panagopoulos and T. Xiang, Phys. Rev. Lett. **81**, 2336 (1998).
[23] K. McElroy *et al.*, Phys. Rev. Lett. **94**, 197005 (2005).
[24] G. Kotliar and J. Liu, Phys. Rev. B **38**, R5142 (1988).